Effects of the Dielectric Environment on Electronic Transport in Monolayer MoS_2: Screening and Remote Phonon Scattering

Maarten L. Van de Put*, Gautam Gaddemane†, Sanjay Gopalan, and Massimo V. Fischetti
Department of Materials Science and Technology, *The University of Texas at Dallas*, Richardson, Texas, USA
*Email: maarten.vandeput@utdallas.edu
†Now at *imec*, Leuven, Belgium

***Abstract*—We investigate theoretically the impact of the dielectric environment on electronic transport in monolayer MoS_2. In particular, we extend our first-principles Monte Carlo method to account for the screening of the electron-phonon interaction by the free carriers in the layer and the dielectric environment. In addition, we include the effect of remote-phonon scattering induced by the surrounding dielectrics. For monolayer MoS_2 on various dielectric substrates, we find that screening could improve the mobility significantly, but the inclusion of remote-phonon scattering degrades the mobility below its free-standing value. In our model, the introduction of gates in a dual-gate configuration does not appreciably decrease the remote-phonon interaction as it does in inversion layers or thicker films. However, for a double-gate field-effect transistor, we still obtain reasonable transport characteristics.**

I. Introduction

Theoretical models are indispensable for the evaluation of 2D materials as potential channel materials in future field-effect transistors (FETs). Most modeling efforts focus on electronic transport in ideal free-standing layers, neglecting effects of the dielectric environment on the transport characteristics [1]–[9]. However, in experimental configurations and devices, the 2D layer is supported by oxides and often gated and, unlike in bulk materials, the dielectric response in 2D materials is dominated by the environment.

As we will demonstrate, the effects of the dielectric environment (substrates, oxides, gates) lead to significant changes in the mobility of supported 2D materials. Introducing a high-κ dielectric, or increasing the free-carrier concentration, screens the electron-phonon interaction, which improves the transport properties. Conversely, it is also well known that high-κ dielectrics can induce significant remote-phonon scattering that degrades performance. Due to their complex interplay, it is impossible to estimate, *a priori*, the combined effect of screening and remote-phonon scattering.

In this work, we extend our full-band Monte Carlo method for 2D materials [1], [2], to include the two major effects of the dielectric environment: screening and remote-phonon scattering. We briefly touch on the necessary theory and key approximations. We present results for two cases: a suspended monolayer of MoS_2, and a double-gate MoS_2 FET.

This work was supported in part by the Semiconductor Research Corporation (SRC).

II. Theory

A. Screening of the electron-phonon interaction

We incorporate dynamic screening of the electron-phonon interaction by free-carriers and the dielectric environment. To achieve this, we apply a correction to the electron-phonon matrix elements obtained using density functional perturbation theory (DFPT). Neglecting the impact of the exchange and correlation functional, the interaction potential of a phonon mode η (*e.g.*, LA, LO, TA, or TO) for a free-standing layer is given by

$$\delta E_{\rm ep}(\mathbf{r}) \approx \int \mathrm{d}^3 r' \; G^{(0)}(\mathbf{r},\mathbf{r}')\,\delta\rho^{(\eta)}(\mathbf{r}')\,, \tag{1}$$

where $\delta\rho^{(\eta)}$ is the response of the total charge to the phonon mode η, and $G^{(0)}(\mathbf{r},\mathbf{r}')$ is the Green's function of the Poisson equation in vacuum.

For a 2D layer localized at $z=0$ with an effective thickness h, we make the following assumptions:

- Only in-plane ionic displacements are considered, *i.e.*, no flexural modes (ZA / ZO).
- The charge-response to the ionic motion is localized at $z=0$.
- The in-plane phonon wavevector $\mathbf{Q}$ is sufficiently small such that the Green's function is constant over the layer $|z|<h/2$.
- *Umklapp* processes can safely be neglected.

Using these assumptions, we find that the electron-phonon matrix elements are directly proportional to the Green's function of the 2D layer in vacuum $G^{(\rm vac)}_{\mathbf{Q},\omega}(z,z')$. In particular, the matrix elements in vacuum, from a state in band n with in-plane wavevector $\mathbf{K}$ to band m with phonon mode η and in-plane wave-vector $\mathbf{Q}$, can be written as

$$g^{(\rm vac)}_{nm\mathbf{K},\eta\mathbf{Q}} = \sum_{\mathbf{G}\mathbf{G}'} u^*_{m\mathbf{G},\mathbf{K}+\mathbf{Q}} u_{n\mathbf{G},\mathbf{K}} \sum_\alpha \mathrm{e}^{-\mathrm{i}\mathbf{Q}\cdot\boldsymbol{\tau}_\alpha} \times \left(\frac{\hbar}{2M_\alpha\omega^{(\eta)}_{\mathbf{Q}}}\right)^{1/2} \mathbf{e}^{\eta,\alpha}_{\mathbf{Q}}\cdot\boldsymbol{\nabla}_{\boldsymbol{\tau}_\alpha}\rho(\mathbf{Q})\, G^{(\rm vac)}_{\mathbf{Q},\omega^{(\eta)}_{\mathbf{Q}}}(0,0)\,, \tag{2}$$

where $\hbar$ is the reduces Planck constant, $u_{n\mathbf{G},\mathbf{K}}$ are the Fourier components of the Bloch waves with reciprocal lattice vector

$\mathbf{G}$, α indicates the ion at position $\boldsymbol{\tau}_\alpha$ with mass M_α, and $\mathbf{e}_{\mathbf{Q}}^{\eta,\alpha}$ is the polarization vector, and $\omega_{\mathbf{Q}}^{(\eta)}$ is the phonon frequency.

The vacuum Green's function $G_{\mathbf{Q},\omega}^{(\mathrm{vac})}(z,z')$ fully accounts for the dielectric response of the free-standing layer. To account for the dielectric response of the substrate and free-carriers in the layer, as well as boundary conditions imposed by metal gates, we replace $G_{\mathbf{Q},\omega}^{(\mathrm{vac})}(z,z')$ by the complete environment Green's function $G_{\mathbf{Q},\omega}^{(\mathrm{env})}(z,z')$. Since we only need to evaluate at $z=z'=0$, we can simply and efficiently rescale the free-standing electron-phonon matrix elements obtained from DFPT,

$$g_{nm\mathbf{K},\eta\mathbf{Q}}^{(\mathrm{env})} = \frac{G_{\mathbf{Q},\omega}^{(\mathrm{env})}(0,0)}{G_{\mathbf{Q},\omega}^{(\mathrm{vac})}(0,0)}\, g_{nm\mathbf{K},\eta\mathbf{Q}}^{(\mathrm{vac})}\,. \tag{3}$$

In practice, the Green's functions need to be approximated. To account for the dielectric response of the 2D layer, including the response of the free-carrier plasma, we refer the reader to Stern [10] and Maldague [11]. For small Q, the dielectric response of the oxides can be described using the generalized Lyddane-Sachs-Teller form as described in Refs. [12], [13].

B. Remote phonon scattering

When introducing polar substrates and oxides, we have to consider "remote phonon scattering", the interaction of coupled interface-plasmon phonon (IPP) modes with the charge carriers in the channel. The scattering potential is given by the usual Fröhlich-like term [12]. This evaluation requires the calculation of the dispersion of the hybrid IPP modes [13], [14]. Since the complete theory is too elaborate to present here, we refer to the Refs. [12]–[14] for a complete discussion.

In the results shown here, rather than calculating the dispersion of the IPP modes, we have approximated the dielectric response with two LO modes per oxide and have neglected the coupling with the plasmon mode. In this case, the interaction matrix element of mode ν (one of the LO modes) reduces to

$$\left|g_{nm\mathbf{K},\nu\mathbf{Q}}^{(\mathrm{remote})}\right|^2 = \frac{e^2\hbar\omega^{(\nu)}}{2\Omega_{\mathrm{cell}}Q}\left|\frac{1}{\epsilon_{\mathrm{high}}^{(\nu)}} - \frac{1}{\epsilon_{\mathrm{low}}^{(\nu)}}\right|, \tag{4}$$

where $\epsilon_{\mathrm{high}}^{(\nu)}$ is the total dielectric response of the 2D layer and surrounding dielectric environment when mode ν does not contribute, while $\epsilon_{\mathrm{low}}^{(\nu)}$ is the total response where the mode fully responds.

III. Results

We demonstrate the effects of screening and remote phonon interaction on transport through monolayer MoS_2 in two realistic configurations, a supported monolayer and a double-gate FET. The full-band Monte Carlo procedure we use to obtain mobility and FET characteristics has been detailed in Refs. [1], [3], [4]. The electronic band structure, phonon dispersion and free-standing electron-phonon matrix elements we start from have been published in Ref. [3]. The dielectric constant and layer thickness of MoS_2 have been obtained from Ref. [15].

A. Supported MoS_2

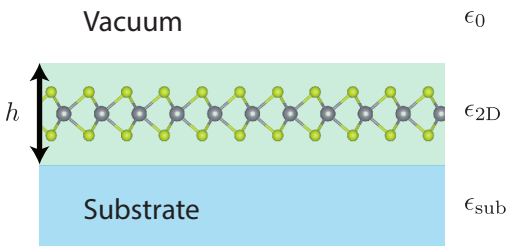

Fig. 1. A supported MoS_2 layer. The layer is supported by an infinitely thick substrate in vacuum. The substrate is either SiO_2, Al_2O_3, and HfO_3. The layer is assumed to have a thickness $h = 6.11\mathring{A}$ and uniform dielectric constant ϵ_{2D}.

We first simulate a supported monolayer of MoS_2 as depicted in Fig. 1. This system is representative of a common experimental setup used to probe the material's "intrinsic" transport characteristics. It is important to note that we consider an idealized, infinitely thick and defect-free substrate that does not change the electronic structure of the MoS_2 layer.

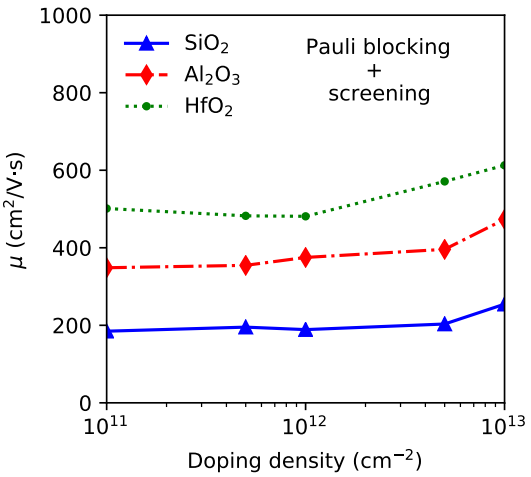

Fig. 2. The screened phonon-limited mobility of the supported MoS_2 layer shown in Fig. 1 with respect to the doping density for various substrates (SiO_2, Al_2O_3, and HfO_3). This includes the screening of the electron-phonon scattering by the substrate.

Figure 2 shows the effect of only free-carrier and dielectric screening on the mobility of a supported layer. For reference, the electron mobility of a free-standing layer, without screening is 127 $\mathrm{cm}^2/(\mathrm{Vs})$ [3]. As expected, the mobility scales with the dielectric constant of the substrate, with higher dielectric constant providing stronger screening of the electron-phonon interactions. Screening by a HfO_2 substrate, the highest κ dielectric we consider, increases the phonon-limited electron mobility of MoS_2 by up to four times, compared to the free-standing material (> 500 $\mathrm{cm}^2/(\mathrm{Vs})$). Even with SiO_2 modest gains are shown, with an electron mobility around 200 $\mathrm{cm}^2/(\mathrm{Vs})$. Considering that our reference point is vac-

uum, the lowest-κ dielectric available, this should not be too surprising.

Looking at the variation of mobility with free-electron concentration (doping), we observe only a marginal improvement in mobility by increasing the doping from 10^{11} cm^{-2} to 10^{13} cm^{-2}. Since the free carriers are confined to the 2D plane of the layer, they cannot efficiently screen the long-wavelength electron-phonon scattering processes. Additionally, we see that degeneracy effects cause variations in the mobility. As the Fermi-level increases, Pauli blocking will result in decreased scattering to already occupied states, increasing mobility. However, with an increasing Fermi level, satellite valleys become available, which increases inter-valley scattering, reducing the mobility. For MoS_2, these degeneracy effects almost cancel each other and do not affect the mobility by appreciably.

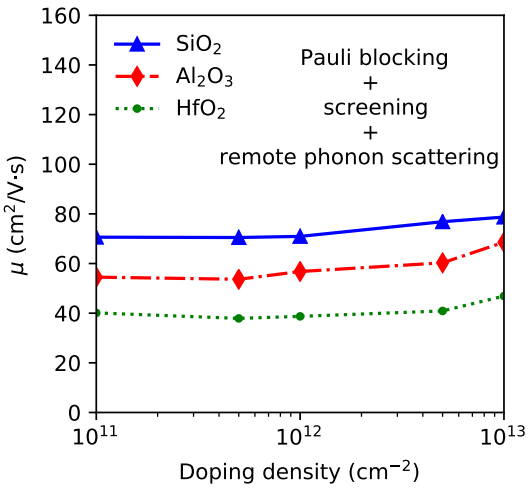

Fig. 3. The screened phonon-limited mobility of the supported MoS_2 layer shown in Fig. 1, including remote-phonon scattering induced by the dielectric with respect to the doping density for various substrates (SiO_2, Al_2O_3, and HfO_3).

While these results may seem promising, Fig. 3 shows that, once remote-phonon scattering is considered, the electron mobility of supported MoS_2 is degraded well below the free-standing mobility for all substrates we consider. Unsurprisingly, HfO_2 shows the largest degradation, reducing the mobility by more than a factor of three to $40\ \mathrm{cm}^2/(\mathrm{Vs})$. Perhaps more surprising, the electron mobility of MoS_2 supported on SiO_2 also drops to $70\ \mathrm{cm}^2/(\mathrm{Vs})$, almost two times lower than the intrinsic mobility of a free-standing layer. It is important to reiterate that this is a common experimental situation when measuring the intrinsic mobility of few-layer 2D materials. Our result suggests that, even under ideal circumstances (no defects or impurities and perfect contacts), the mobility of MoS_2, measured on a substrate, will not exceed $80\ \mathrm{cm}^2/(\mathrm{Vs})$ at room temperature.

B. Double-gate MoS_2 field-effect transistor

To estimate performance in a device, we simulate a MoS_2 FET, as shown in Fig. 4. We consider a double-gate structure

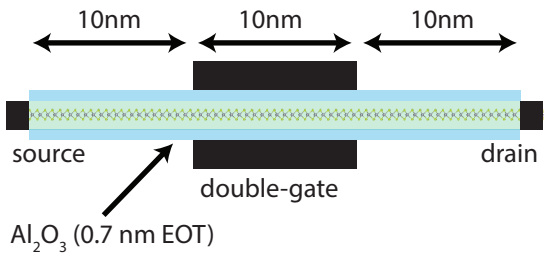

Fig. 4. A double gate MoS_2 FET. The oxide is Al_2O_3, with an equivalent oxide thickness (EOT) of 0.7 nm SiO_2. The lengths of the gate and source/drain extensions are 10 nm each. The channel is undoped, while the source/drain extensions are n-type doped with a concentration of 10^{13} cm^{-2}

with a equivalent oxide thickness (EOT) of 0.7 nm SiO_2.

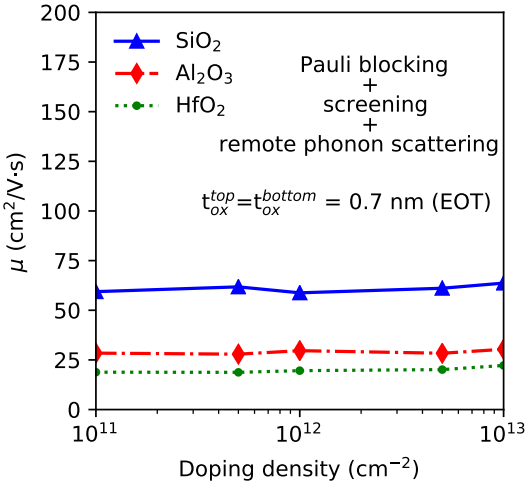

Fig. 5. The screened phonon-limited mobility of the supported MoS_2 layer shown in Fig. 1, including remote-phonon scattering induced by the dielectric with respect to the doping density for various substrates (SiO_2, Al_2O_3, and HfO_3).

Looking at the channel region, Fig. 5 shows the mobility in the presence of various oxides in the double gate configuration. While creening is much stronger (not shown) in this configuration, adding an additional oxide doubles the number of remote-phonon branches and causes a net reduction in mobility in the channel for all oxides. We note that, unlike in bulk materials, screening by the metal gates only has a limited effect on suppressing the remote-phonon interaction. Indeed, in our model we consider the charges in the layer extremely confined, evaluating the remote-phonon interaction only at a single point in the center, which is not sensitive to screening by the gates. Whereas, in reality, the effect of the gates will be larger. Presumably, screening by the metal gates will be far less efficient in 2D materials than in (bulk) inversion layers or thick films due to the highly confined nature of the former.

For Al_2O_3, we perform fully self-consistent calculations on the FET structure shown in Fig. 4. Screening and remote phonon interaction are automatically updated to account for the local charge distribution and geometry. Figure 6 shows the

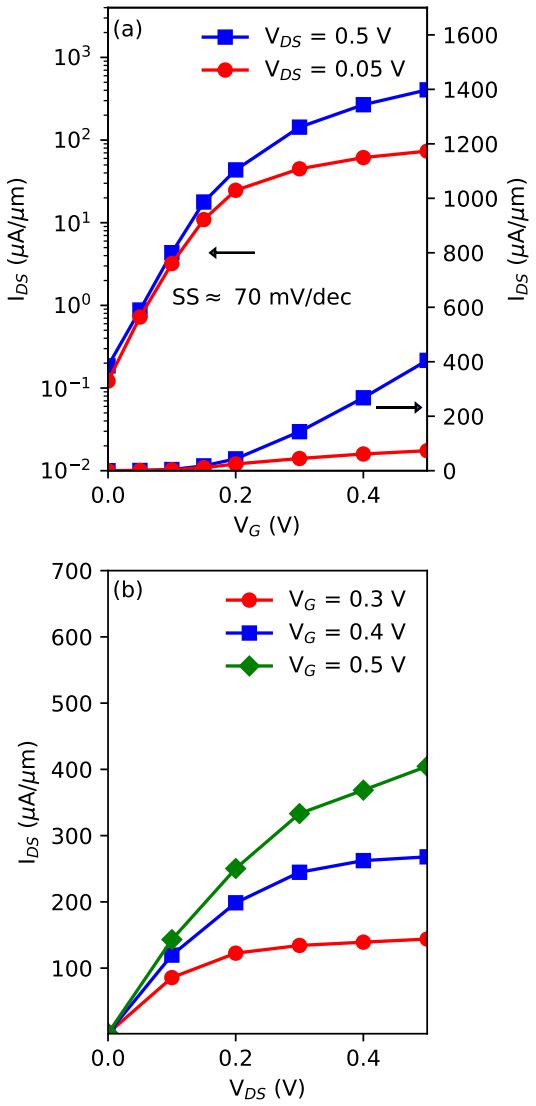

Fig. 6. Transfer (a) and output (b) characteristics of the device shown in Fig. 4, including all screening effects and remote phonon scattering.

transfer and output characteristics of the FET. When accounting for remote-phonon scattering, the transport characteristics compare favorably to state-of-the-art experimental results [16]. Compared to the mobility calculations of supported and gated MoS_2, the device characteristics are promising. Indeed, it is well known that in short devices that mobility is not a good measure for FET performance. Therefore, to design an optimized FET configuration, *e.g.*, materials selection and geometry, complete Monte-Carlo calculation including these effects are required.

IV. Conclusions

The effects of the dielectric environment on the mobility of 2D materials cannot be neglected. While dielectric screening can significantly improve the mobility, these positive effects are countered by the detrimental effect of remote-phonon scattering. For now, the only way to know to which side the balance will tip is to diligently study the transport properties using models that include the interactions with the dielectric environment. Since experimental measurements on supported layers and FETs are inherently affected by all of these physical processes, direct comparison to theoretical values in free-standing layers is perilous. From a device engineering perspective, the choice of the right material *combination* is essential, a task for which advanced modeling, as shown here, is crucial.

References

[1] G. Gaddemane, W. G. Vandenberghe, M. L. Van de Put, S. Chen, S. Tiwari, E. Chen, and M. V. Fischetti, "Theoretical studies of electronic transport in monolayer and bilayer phosphorene: A critical overview," *Physical Review B*, vol. 98, p. 115416, Sep 2018.

[2] G. Gaddemane, W. G. Vandenberghe, M. L. Van de Put, E. Chen, and M. V. Fischetti, "Monte-Carlo study of electronic transport in non-σ_h-symmetric two-dimensional materials: silicene and germanene," *Journal of Applied Physics*, vol. 124, no. 4, p. 044306, 2018.

[3] G. Gaddemane, S. Gopalan, M. L. Van de Put, and M. V. Fischetti, "Limitations of ab initio methods to predict the electronic-transport properties of two-dimensional semiconductors: the computational example of 2H-phase transition metal dichalcogenides," *Journal of Computational Electronics*, vol. 1, p. 3, jun 2020.

[4] G. Gaddemane, M. L. V. de Put, W. G. Vandenberghe, E. Chen, and M. V. Fischetti, "Monte carlo analysis of phosphorene nanotransistors," *arXiv:2007.14940*, 2020.

[5] S. Gopalan, G. Gaddemane, M. L. Van de Put, and M. V. Fischetti, "Monte carlo study of electronic transport in monolayer InSe," *Materials*, vol. 12, no. 24, p. 4210, Dec 2019.

[6] T. Sohier, M. Calandra, and F. Mauri, "Two-dimensional fröhlich interaction in transition-metal dichalcogenide monolayers: theoretical modeling and first-principles calculations," *Phys Rev B*, vol. 94, p. 085415, Aug 2016.

[7] T. Sohier, D. Campi, N. Marzari, and M. Gibertini, "Mobility of two-dimensional materials from first principles in an accurate and automated framework," *Phys. Rev. Materials*, vol. 2, p. 114010, Nov 2018.

[8] Y. Lee, S. Fiore, and M. Luisier, "Ab initio mobility of single-layer MoS_2 and WS_2: comparison to experiments and impact on the device characteristics," in *2019 IEEE International Electron Devices Meeting (IEDM)*, 2019, pp. 24.4.1–24.4.4.

[9] C. Klinkert, Á. Szabó, C. Stieger, D. Campi, N. Marzari, and M. Luisier, "2-D materials for ultrascaled field-effect transistors: one hundred candidates under the ab initio microscope," *ACS Nano*, vol. 14, no. 7, pp. 8605–8615, 2020, pMID: 32530608.

[10] F. Stern, "Polarizability of a two-dimensional electron gas," *Physical Review Letters*, vol. 18, pp. 546–548, Apr 1967.

[11] P. F. Maldague, "Many-body corrections to the polarizability of the two-dimensional electron gas," *Surface Science*, vol. 73, pp. 296 – 302, 1978.

[12] M. V. Fischetti, D. A. Neumayer, and E. A. Cartier, "Effective electron mobility in Si inversion layers in metal-semiconductor systems with a high-κ insulator: The role of remote phonon scattering," *Journal of Applied Physics*, vol. 90, no. 9, pp. 4587–4608, 2001.

[13] Z.-Y. Ong and M. V. Fischetti, "Theory of remote phonon scattering in top-gated single-layer graphene," *Physical Review B*, vol. 88, p. 045405, Jul 2013.

[14] ——, "Theory of interfacial plasmon-phonon scattering in supported graphene," *Physical Review B*, vol. 86, no. 16, p. 165422, Oct 2012.

[15] A. Laturia, M. L. Van de Put, and W. G. Vandenberghe, "Dielectric properties of hexagonal boron nitride and transition metal dichalcogenides: from monolayer to bulk," *npj 2D Materials and Applications*, vol. 2, no. 1, p. 6, dec 2018.

[16] Q. Smets, G. Arutchelvan, J. Jussot, D. Verreck, I. Asselberghs, A. N. Mehta, A. Gaur, D. Lin, S. E. Kazzi, B. Groven, M. Caymax, and I. Radu, "Ultra-scaled MOCVD MoS_2 MOSFETs with 42nm contact pitch and 250μa/μm drain current," in *2019 IEEE International Electron Devices Meeting (IEDM)*, 2019, pp. 23.2.1–23.2.4.